Available online at www.sciencedirect.com
ScienceDirect
International Journal of Multiphase Flow 34 (2008) 128–144
International Journal of Multiphase Flow
www.elsevier.com/locate/ijmulflow

Experiments on two-phase flow distribution inside parallel channels of compact heat exchangers

A. Marchitto, F. Devia, M. Fossa, G. Guglielmini *, C. Schenone

Diptem, University of Genoa, Via all'Opera Pia 15A, 16145 Genoa, Italy

Received 14 February 2007; received in revised form 16 July 2007

Abstract

Uneven distribution in heat exchangers is a cause of reduction in both thermal and fluid-dynamic performances. Many papers have dealt with single-phase flow and both flow distribution data and analytical or numerical models are available for header design. With regard to two-phase flow, phase separation in manifolds with several outlets is so complicated that, to date, there is no general way to predict the distribution of two-phase mixtures at header-channel junctions. The design of headers for new generation compact heat exchangers and multi-microchannel evaporators is still based on an empirical approach, as a number of variables act together: geometrical parameters and orientation of the manifolds and of the channels, operating conditions, fluid physical properties.

In the present paper measurements of the two-phase air–water distributions occurring in a cylindrical horizontal header supplying 16 vertical channels are reported for upward flow. The effects of the operating conditions, of the header-channel distribution area ratios and of the inlet port orifice plates were investigated. The flow rates of each phase flowing in the different channels were measured. Time varying, void fraction data were also analysed to characterise the two-phase flow patterns. Video records were taken in order to infer different flow patterns (from intermittent to annular) inside the header-channel system.

Keywords: Flow distribution; Air–water mixture; Parallel channels; Plate heat exchangers; Orifice plates

1. Introduction

One of the factors that most strongly influence the performance of compact heat exchangers is the degree of flow rate uniformity in the various parallel channels where the heat transfer occurs.

Plate heat exchangers (PHE) have long been used in a wide range of industrial applications regarding single-phase flow. Recently, two-phase gas/liquid mixtures have been utilized in such exchangers in processes involving vaporisation and condensation. Typical examples include refrigerating cycles, in which the use of such components favours compactness and improves heat transfer performance. Multi-microchannel tube

* Corresponding author. Tel.: +39 0103532877; fax: +39 010311870.
E-mail address: guglielm@ditec.unige.it (G. Guglielmini).

0301-9322/$ - see front matter © 2007 Elsevier Ltd. All rights reserved.
doi:10.1016/j.ijmultiphaseflow.2007.08.005

heat exchangers are also relatively common and especially in mobile air-conditioning applications. Interest in micro-channel heat exchangers is keen, owing to their compactness, which saves space, weight and refrigerant charge.

Both evaporators and condensers raise the problem of ensuring uniform distribution of the two-phase flow from the distributor to the multi-channel system that makes up the exchanger. Uneven two-phase distribution can occur both inside each channel, owing to the asymmetrical parallel and diagonal flow, and inside the header, owing to the separation of the two-phase mixture in the header-tube junctions.

Flow mal-distribution in heat exchangers may be spatial, temporal or both, its effect being to reduce both thermal and fluid-dynamic performances. Many papers have dealt with the effects of flow mal-distribution on the performance of heat exchangers (Mueller, 1987; Mueller and Chiou, 1988; Probhakara Rao et al., 2005). Some mal-distributions are the result of fabrication conditions, such as mechanical design or manufacturing tolerances; others are caused by the heat transfer and fluid flow process itself, by fouling and/or corrosion, or by the typical non-uniformities of two-phase flows. The effects on heat transfer efficiency and operating control vary. While some cases of bad distribution have little effect on heat exchanger performances, others result in significant loss of performance and/or mechanical failure of the devices (Mueller and Chiou, 1988). For these reasons, several recent studies have analysed the effects of geometrical configuration and operating conditions on the distribution of two-phase flows.

The present paper reports the results of several experiments carried out on a cylindrical horizontal two-phase flow header supplying upwardly oriented sixteen vertical channels. The aim of this work is to analyse the effects on two-phase distribution of orifice plates placed upstream of the header and perforated plates connecting it to the channels. Although these configurations are widely used in real distributors, they have not been extensively studied in the literature. Measurements of air–water flow rate distributions were taken for a number of operating conditions and for different geometrical configurations. Time varying, cross-sectional void fraction data were analysed to characterise the two-phase flow patterns in the header section. Video records were taken in order to infer the flow patterns inside the distributor during intermittent and almost annular flows.

2. Previous works

With regard to single-phase flow, many papers have been published on flow distribution data and analytical and numerical models for manifold design. Among the early works, Acrivos et al. (1959) obtained an iterative solution for viscous, single-phase flow in headers. Bajura and Jones (1976) studied flow distribution in lateral branches of different manifolds, both analytically and experimentally. They showed that uniform flow distribution in the lateral branches is attained only when the headers act as infinite reservoirs. Bassiouny and Martin (1984) attempted to find a correlation between the header geometry and the flow distribution. Kim et al. (1995) investigated the effects of header shapes and the Reynolds number in a parallel-flow manifold to be used in a liquid module for electronic packaging. They found that the flow distribution depended sensibly on the header shape and on the Reynolds number. Yin et al. (2002) experimentally studied the pressure drops inside the complex headers and parallel circuits of a micro-channel heat exchanger. A pressure drop model for the whole heat exchanger was developed and the pressure and mass flow rate distribution inside the heat exchanger were predicted.

Two-phase flow distribution from a header to parallel channels gained great attention to predict the heat transfer performance of compact heat exchangers, evaporators and condensers. The distribution of two-phase mixtures through the channels is often non-uniform, and in extreme cases there is almost no liquid flow through some channels. In evaporators, uniform distribution is essential in order to avoid dry-out phenomena and the resulting poor heat exchange performance. In condensers, uneven distribution of liquid could create zones of reduced heat transfer due to high liquid loading. Thus, in designing compact heat exchangers, understanding separation phenomena in the manifolds is of great importance.

The two-phase flow structure in compact heat exchangers is very complex and to date there is no general way to predict the distribution of the two-phase mixtures at the header-channel junctions. In fact many variables act together, such as the geometric factors (manifold shape, channel junctions, flow orientation) and the

operating conditions (mass flow rate and vapour quality at the inlet of the distributors and heat load on the tubes).

Several authors have investigated two-phase flow division in T-junctions. However, phase separation in manifolds is so complicated that T-junction findings cannot be directly applied to the study of a multi-channel system (Watanabe et al., 1995). Only a limited number of studies have investigated the complex phenomena that occur in two-phase flow distributors.

A few studies have attempted to identify an appropriate CFD model for refrigerant distributors (Li et al., 2002a,b). Experiments were performed that aimed to validate the general trends associated with the CFD results. However, it is important to note that the systems studied were characterised by only a few branches and by operating conditions that could be well represented by the homogeneous flow model.

Most studies on two-phase distribution in compact heat exchangers have been experimental. Our literature search is summarized in Table 1, which includes the description of test geometry, experimental conditions and two-phase mixtures used.

Generally speaking, experiments have been performed under adiabatic conditions. Only Vist and Pettersen (2004) investigated the influence of changing the heat flux to the evaporator tubes on the two-phase distribution in the manifold. Changing the heat load on the evaporator test section had little influence on the two-phase flow distribution, while the two-phase flow distribution markedly influenced the heat exchanged between the refrigerant and the counter-flowing water. All found studies used air–water mixtures or halocarbon refrigerants. Rong et al. (1996) used air–water mixtures to simulate an R-134a refrigerant system at the same inlet volumetric flow rates. Webb and Chung (2005) simulated the actual refrigerant flow conditions by means of air–water mixtures with the same liquid–vapour density ratio and the same Martinelli parameters (Xtt).

Operating conditions varied from bubbly and slug flows (Osakabe et al., 1999; Horiki and Osakabe, 1999) to annular flow (Lee and Lee, 2004) at the header inlet.

Lee recently presented an extensive review (2006) of research on two-phase distribution in dividing tubes and parallel channels. A review of experimental and theoretical studies was also presented by Guglielmini (2006). The effects of tube outlet direction, tube protrusion depth, mass flow rate and quality were experimentally investigated by Kim and Sin (2006) for a horizontal round header and 30 vertical flat tubes simulating a parallel-flow heat exchanger; both upward and downward flow were considered. For flush-mounted configurations, their results confirmed what other researchers had found: downward flow and upward flow led water to flow mostly through the front and rear parts of the header, respectively. The effect of tube protrusion depth was also studied: for the downward flow configuration, as protrusion depth was increased, more water was forced to the rear part of the header, while for the upward flow configuration, the flow distribution was not significantly altered. A negligible difference in two-phase flow distribution was observed between the parallel and the reverse-flow configurations.

In recent years, several studies have been devoted to the comprehension of the flow field in manifolds connecting a series of micro-channels (Beaver et al., 2000; Tomkins et al., 2002; Hrnjak, 2004; Fei et al., 2002; Cho et al., 2003; Fei and Hrnjak, 2004). These studies have been performed by using either air–water mixtures or various refrigerants (e.g. R22, R134a, R744). The main parameters examined have been the orientation of the header (horizontal or vertical) the flow direction of the refrigerant into the inlet header (in-line, parallel and cross-flow) and operating conditions. Most studies have confirmed the difficulty of obtaining uniform two-phase flow distribution. The distribution of the fluid into each parallel micro-channel tube is a function of the flow regime in the header. However, it is also significantly affected by the type of connection between the pipes and the header, the shape of the inlet port, the protrusion depth, the orientation, etc.

Experiments on two-phase flow distribution have demonstrated that, among the main factors affecting the splitting of the phases, a very important role is played by the various geometric factors involved: distributor shape and size, channel junctions, header and channel orientation, the size and length of the inlet pipe, and the intrusion depth of the channels into the header wall. All these parameters can strongly affect the distribution of gas and liquid flow rates among the channel pipes. However, the behaviour can be completely changed by particular upstream conditions, such as the presence of fittings (e.g. nozzles or short inlet tubes), which are able to modify the two-phase flow pattern at the inlet of the manifold. As Webb and Chung (2005) concluded, the design of devices to improve the distribution is nowadays ‘‘highly empirical’’.

Table 1
Literature studies on two phase flow distributors

Ref.	Fluids	Operating conditions	Inlet straight pipe diameter/length (mm)	Header orientation/ channel flow direction	Header cross section/ hydraulic diameter/ length (mm)	Channel cross section/ hydraulic diameter/ length (mm)	Channel pitch/ channel intrusion depth (mm)
Bernoux et al. (2001)	R-113	$\dot{m}'' = 35$–100 $x = 0.1$–0.8	17.3/100	HH/VDC	C/50/96	SQ/3.85/50	10/0
Cho et al. (2003)	R-22	$\dot{m}'' = 60$ $x = 0.1$–0.3	/	VH and HH/multi-microchannels	/19.4/148	SQ ($D_h = 1.32$ mm)/622	/0
Fei et al. (2002)	R-134a	$\dot{m}'' = 0.02$–0.06 $x = 0$–0.3	10/120	HH/VDC	/ /67	/ / /	/
Horiki and Osakabe (1999)	Water–air	$V_{SL} = 0.054$–0.1 $Re_L = 2000$–4000	/600	HH/VUC	SQ/40/	/10/1000	130/0; 20; 30
Kim and Sin (2006)	Water–air	$\dot{m}'' = 70$–200 $x = 0.2$–0.6	/1000	HH/VDC and VUC	/17/	SQ/1.23/910	/0; 4.25 (0.25D); 8.5 (0.5D)
Lee and Lee (2004)	Water–air	$\dot{m}'' = 54$–134 $x = 0.2$–0.5	SQ 24×24/1650	VH upward/HC	SQ/24/	SQ/3.33/500	9.8/0; 6; 12
Osakabe et al. (1999)	Water–air	$V_{SL} = 0.054$–0.1 Small bubbles $Re_L = 2000$–4000	/600	HH/VUC	SQ/40/	/10/585, 800, 1000	130/0
Rong et al. (1996)	Water–air	$V_{SL} = 0.015$–0.241 $V_{SG} = 4.48$–32.19	/	Two types of evaporator plates/vertical U and inverted U channels	C/ /	Single and multiple channels between plates/ / 183	/0
Taitel et al. (2003)	Water–air	$G_L = 0.1$–3 $G_G = 0.05$–3	/	Inlet and outlet HH/IC	/50/	/26/6000	600/0
Tomkins et al. (2002)	Water–air	$\dot{m}'' = 50$–400 $x = 0$–0.4	/	HH/VDC	SQ/280×3.75–12.7/560	C/1.59/317.5	/0

(*continued on next page*)

Table 1 (*continued*)

Ref.	Fluids	Operating conditions	Inlet straight pipe diameter/length (mm)	Header orientation/ channel flow direction	Header cross section/ hydraulic diameter/ length (mm)	Channel cross section/ hydraulic diameter/ length (mm)	Channel pitch/ channel intrusion depth (mm)
Vist and Pettersen (2004)	R-134a	$\dot{m} = 0.025$–0.042 $x = 0.11$–0.5 $T = 40, 50, 60$	16/250	HH/VUC and VDC	C/8 or 16/	C/4/	21/0
Watanabe et al. (1995)	R-11	$\dot{m}'' = 40$–120 (vertical) 440–620 (horizontal) $x = 0$–0.3	/	HH/VUC; VH/HC	Vertical type: /20/ Horizontal type: /6/	C/6/	/0
Webb and Chung (2005)	Water–air	$\dot{m}_L = 36.01$–189.19 $\dot{m}_G = 87.8$–240.99	/	HH/rectangular VC	D-shaped cross section/32/	SQ/1.3/750	2.2/4
Yin et al. (2002)	N_2	$\dot{m} = 0.001$–0.02	7/250	Heat exchanger with microchannel tubes	C/7/465	/0.787/815	/0

Note: $\dot{m}''$: mass flux (kg/m^2 s), x: mass quality (–); Re_L: Reynolds number (–); V_{SL}: liquid superficial velocity (m/s); V_{SG}: gas superficial velocity (m/s); G_L: liquid volumetric flow rate (l/s); G_G: gas volumetric flow rate (l/s); $\dot{m}$: flow rate (kg/h); $\dot{m}_L$: liquid flow rate (kg/h); $\dot{m}_G$: gas flow rate (kg/s); T: temperature (K); HH: horizontal header; VH: vertical header; VDC: vertical downward channels; VUC: vertical upward channels; HC: horizontal channels; IC: inclined channels; C: circular; R: rectangular; SQ: square.

A further confirmation of this condition is the point that, whereas orifices and nozzles are commonly used by heat exchanger manufacturers to empirically adjust the flow rate distribution on the basis of the operating conditions and of the unit dimension, these aspects have not yet been sufficiently investigated, and no systematic study is reported in the literature. The aim of the experimental campaign is therefore to deeply study some phenomenological aspects of the two-phase flow separation produced either by varying the area restriction caused by thin orifice plates (between the straight pipe and the distributor) or by varying the header-channel area ratios at the connection of the header to the parallel channels by inserting perforated plates of different sizes.

3. Experiments

Experiments were carried out on a simple test section in order to investigate some phenomenological aspects of the two-phase distribution in compact heat exchanger manifolds. The flow inside the vertical channels was upward. The test section was designed to allow the visualisation of flow structure in the inlet port and inside the header. The instrumentation was designed to record the pressure and void fraction evolution inside the header and to measure the liquid and gas flow rates insides the parallel channels, downstream of the header.

3.1. Experimental set-up and procedure

This experimental apparatus consists of two supply lines of air and water that merge into a horizontal pipe (Fig. 1). Phase mixing (through a T fitting) allows intermittent and annular flow regimes to be generated. Downstream of the mixer, the mixture flows horizontally inside a 2.0 m long acrylic pipe with an inner diameter of 26 mm. The pipe is connected by a flange to the inlet port of the test section. An overall sketch of the experimental apparatus is given is Fig. 1.

Downstream of the test section, an array of valves can operate in order to extract the flow rate coming from a pair of vertical channels and to divert it toward the extraction phase separator, which carries the liquid and gas phases toward the corresponding flow meters: the air is then released into the atmosphere, while the water is pumped to the water reservoir, which also acts as the main separator. The other two-phase streams that

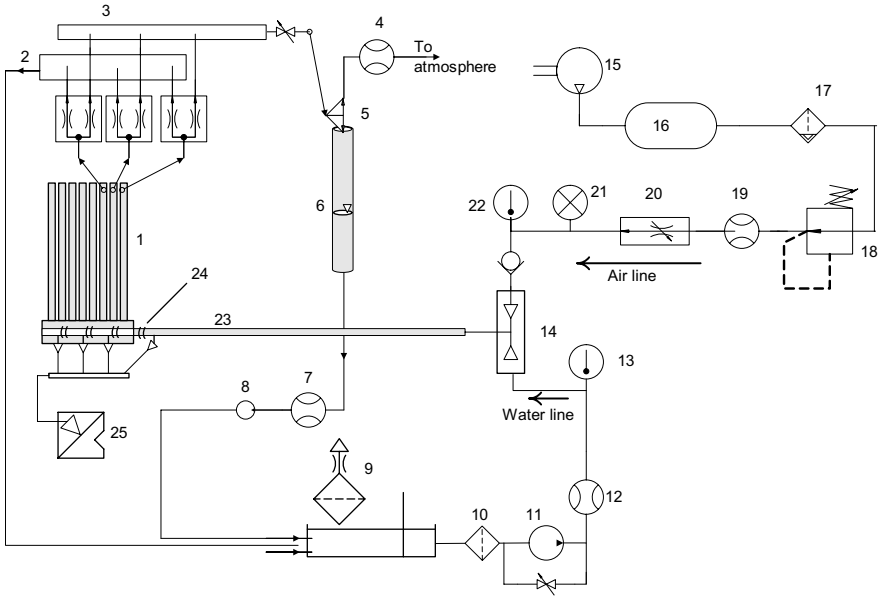

1: Test section
2: Main collector
3: Extraction collector
4: Extracted gas flow meter
5: Extraction separator
6: Phase separator
7: Extracted liquid flow meter
8: Extraction pump
9. Water reservoir
10: Water filter
11: Main pump
12: Main liquid flow meter
13: Liquid temperature meter
14: Mixer
15. Air compressor
16. Air Reservoir
17: Air filter
18: Pressure regulator
19: Main gas flow meter
20: Gas flow regulation (gate valve)
21: Pressure gauge
22: Gas temperature
23: Transparent pipe
24: Impedance probe (S_1)
25: Pressure transducer

Fig. 1. Schematic drawing of the flow loop.

depart from the test section outlet ports are sent, via flexible hoses, to the main separator. The loop is closed at the mixing junction, where the air coming from the air supply line and the water pumped by the main pump are mixed to generate the two-phase flow.

Characterization of the operating conditions and investigation of phase distribution inside the pair of channels are based on the measurement of the gas and liquid flow rates. The main and extracted gas streams are metered by two thermal devices, able to directly measure the mass flow rate with an overall accuracy of ±2% of the reading. The main and extracted liquid streams are metered by two magnetic devices with an overall accuracy of ±0.8% of the reading. In order to deduce the inlet gas superficial velocity, local pressure and temperature must be known. The gas temperature is measured by a K-type thermocouple connected to a rack display, which converts the signal into a 4–20 mA current for the acquisition system. The overall accuracy of temperature measurement is ±1 °C. Additional measurements are those water temperature (by a K-type thermocouple) and the gas pressure after the pressure regulator, upstream of the mixer, by an absolute pressure transducer.

The test section (Fig. 2) consists of a distributor, an interchangeable orifice plate and a system of $n = 16$ vertical channels. The upper outlet ports of the channels are connected in pairs in order to allow the stream from each pair to be separately collected (channel pairs from $j = 1$ to $j = 8$). The distributor has a circular cross-section of $D = 26$ mm i.d and was machined and polished from a rectangular block of acrylic resin. The transparent block facilitates visualisation, while the flat external surface minimises the distortion due to refraction. Horizontally oriented, the distributor is equipped with an interchangeable plate with 16 orifices supplying an equal number of vertical channels, which are connected to the header with a pitch of 18 mm (Fig. 2). The channel dimensions (length, depth, width) are 500, 15, 18 mm, respectively. The flange connecting the header to the upstream supply pipe can be fitted with an orifice plate (inlet nozzle), in order to investigate the remixing effects of such singularity on the flow distribution inside the header and the channels. Four pressure taps (connected to a differential pressure transducer) allow the pressure gradient at the header inlet, and inside it, to be recorded.

Four impedance probes are simultaneously used to obtain the instantaneous cross-sectional void fraction upstream the distributor and inside it. The void fraction sensor adopted in this investigation consists of ring

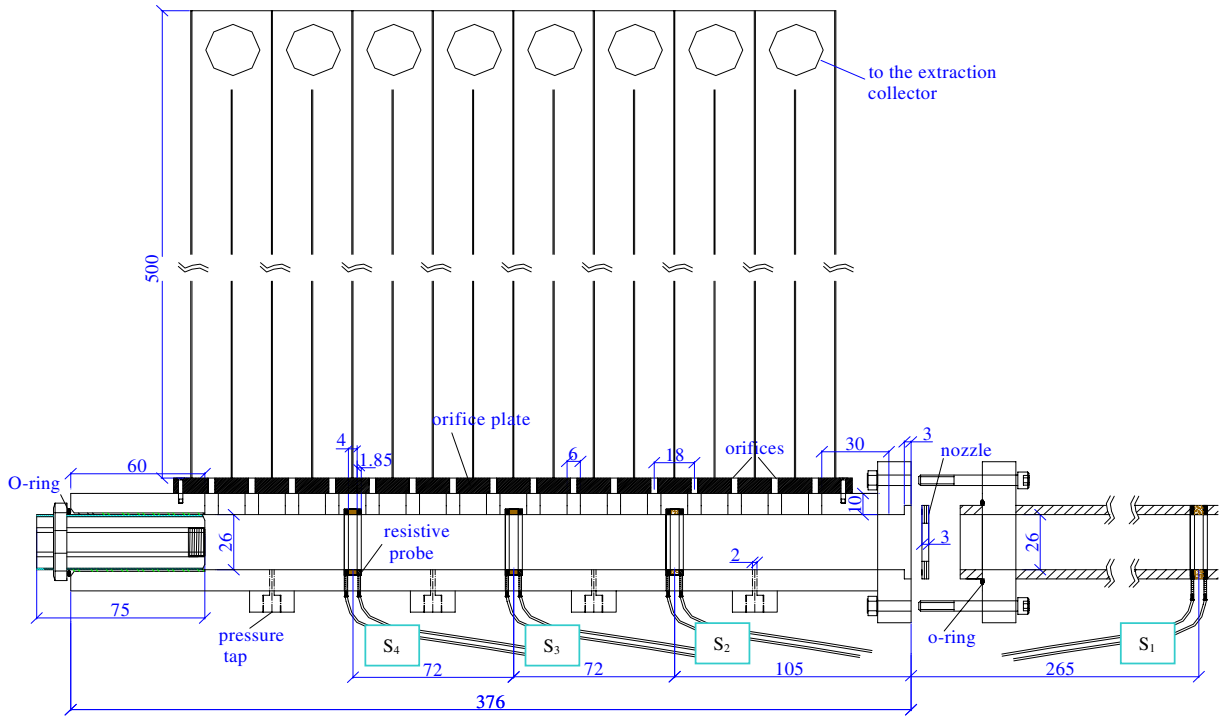

Fig. 2. Schematic diagram of the test section.

electrode pairs placed on the internal wall of the cylindrical test duct, flush to the pipe surface; one sensor (S1) is placed upstream of the distributor, 10.6 diameters upstream of the inlet port, and the other three sensors (S2, S3 and S4) are placed inside the distributor, equally spaced 72 mm apart.

The description of the procedure and the uncertainty analysis on void fraction measurement have been reported elsewhere (Fossa, 2001; Fossa and Guglielmini, 2002), the uncertainty being found to be about 4%. From the analysis of the probe signal, the time-average cross-sectional void fraction $\bar{\alpha}$ and the void fraction probability density function (PDF) can be inferred; this latter is a key figure in flow pattern identification (Zuber and Jones, 1975).

3.2. Geometrical factors and operating conditions

The experiments were carried out for different flow conditions and for different geometrical configurations. The operating conditions, evaluated at the distributor inlet, cover the $V_{sg} = 1.50$–16.50 m/s and $V_{sl} = 0.20$–1.20 m/s, gas and liquid superficial velocity ranges, respectively. Intermittent flows (plug, slug) and annular flow were visually observed. Analysis of the PDFs of the void fraction signals (as obtained from the probe upstream of the inlet port section) and the inspection of the Taitel and Dukler (1976) map confirmed the existence of intermittent and annular flow regimes (Fig. 3). The pressure at the test section inlet was varied in the range from 1.4 to 2.2 bar to control the superficial velocities, also taking into account the pressure drops through the orifice plate and the nozzle, when present.

At the connection of the header to the parallel channels, four different orifice plates with the diameter δ of 2, 3, 4 and 6 mm, were employed. The resulting four different header-channel area ratios $A_R = \frac{1}{n}(D/\delta)^2$ were 10.56, 4.69, 2.64 and 1.17, respectively. The straight pipe and the distributor were connected either by orifice nozzles (20, 16 and 12 mm i.d.) or without any area restriction ($\sigma = (d/D)^2 = 1$).

3.3. Data processing

The gas and liquid flow rates measured are hereafter presented in a non-dimensional way. The non-dimensional gas flow ratio ($\dot{m}^*_{g,j}$) or liquid flow ratio ($\dot{m}^*_{l,j}$) inside the pair of channels No. j is the ratio of the measured gas or liquid flow rate ($\dot{m}_{k,j}$) in the pair of channels under consideration (No. j) over the mean gas (or liquid) flow rate calculated for uniform distribution:

$$\dot{m}^*_{k,j} = \frac{\dot{m}_{k,j}}{\sum_{i=1}^{N} \dot{m}_{k,i}/N} \quad (k = g, l)$$

where N is the overall number of channel pairs.

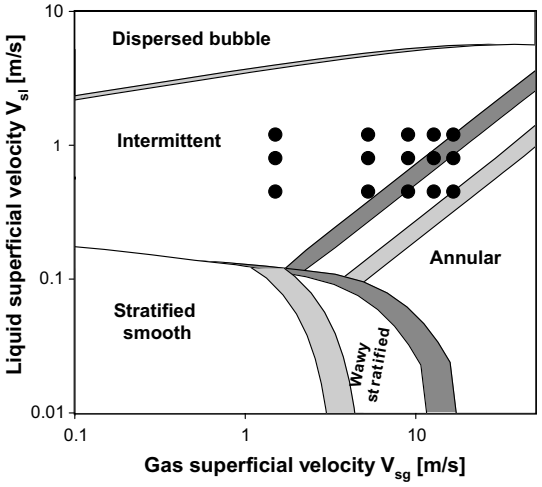

Fig. 3. Flow patterns at the distributor inlet on Taitel and Dukler (1976) map.

Further physical quantities were measured: the instantaneous value of the cross-sectional void fraction at the inlet port and inside the header, the absolute pressure and the temperature at the inlet port.

From the statistical analysis of the void fraction time series, information was inferred on the actual two-phase flow pattern at the inlet and inside the header. The absolute pressure and the temperature at the inlet port were used as references to obtain the local gas and liquid superficial velocities.

The phase distributions inside the channels were also analysed in terms of the standard deviation of the k-phase flow ratio, here defined as follows:

$$\mathrm{STD}_k = \sqrt{\sum_{j=1}^{N} (\dot{m}^*_{k,j} - 1)^2 / N}$$

For every geometrical configuration and operating condition STD_k represents a synthetic, single-value, index of liquid or gas flow rate mal-distribution. When local gas or liquid flow rate is close to the mean calculated value, STD_k is small and tends to increase as the flow distribution worsens.

A further index was then introduced to analyse and quantify flow rate mal-distribution: NSTD_k indicates the "Normalized Standard Deviation" for the k-phase, which is the ratio between the actual STD_k and the maximum value of standard deviation for a certain number, N, of vertical channels.

$$\mathrm{NSTD}_k = \frac{\mathrm{STD}_k}{\mathrm{STD}_{k,\max}} = \sqrt{\frac{\sum_{j=1}^{N} (\dot{m}^*_{k,j} - 1)^2}{(N-1)N}}$$

By utilizing STD or NSTD for both phases it is possible to compare the uniformity of gas and liquid flow rate for different conditions, thus determining the relative effectiveness of the various configurations investigated. Several other indexes can be used to synthetically rank the behaviour of header-channels systems with regard of flow rate distribution. Here, STD and NSTD were chosen because of their simplicity and because STD was previously utilized by other authors (Vist and Pettersen, 2004; Hrnjak, 2004; Fei et al., 2002; Cho et al., 2003; Fei and Hrnjak, 2004) for similar analysis.

4. Results and discussion

4.1. Effects of the operating conditions on two-phase flow distributions

The distribution of the mass flow rate of each phase among the channels, for a given geometrical configuration, strongly depended on the superficial gas and liquid velocities at the header inlet.

Typical distribution profiles at low values of the liquid superficial velocity ($V_{sl} = 0.45$ m/s) are presented in Fig. 4a and b, in terms of gas and liquid flow ratios, respectively, with the gas superficial velocity as a parameter. The orifice diameter δ in these representations is 4 mm ($A_R = 2.64$) and in these cases no inlet nozzle is present ($\sigma = 1$). At the lowest gas superficial velocity ($V_{sg} = 1.50$ m/s), the gas phase was mainly diverted into the first channel pairs, promoting a rush of water into the first three pairs of channels, while the liquid flow ratio decreased below the value of 1 in the remaining channels. The liquid flow ratio was characterised by a maximum, which tended to move toward the downstream channels as the gas flow rate increased. At higher values of the gas superficial velocity, the gas flow rate tended to become more uniform, while the water flow rate tended to feed only the last pairs of channels. All these behaviours are well described in Fig. 4c, in which the liquid flow ratios are reported as a function of gas superficial velocity of the mixture for each pair of channels. The situations corresponding to $V_{sl} = 0.45$ m/s, $V_{sg} = 1.50$ and 5.25 m/s are also reproduced in the images in Fig. 5, in which the different flow patterns and the phase distributions in each channel are clearly visible.

At the liquid superficial velocity of $V_{sl} = 1.20$ m/s, the gas and liquid phases were again unevenly distributed. In this case, however, the gas phase was preferentially distributed into the first channels, while the liquid phase was generally distributed into the last channels, even at low gas superficial velocities. On increasing the gas flow rate, the gas flow ratio profile improved, thus reducing the mal-distribution. By contrast, the liquid

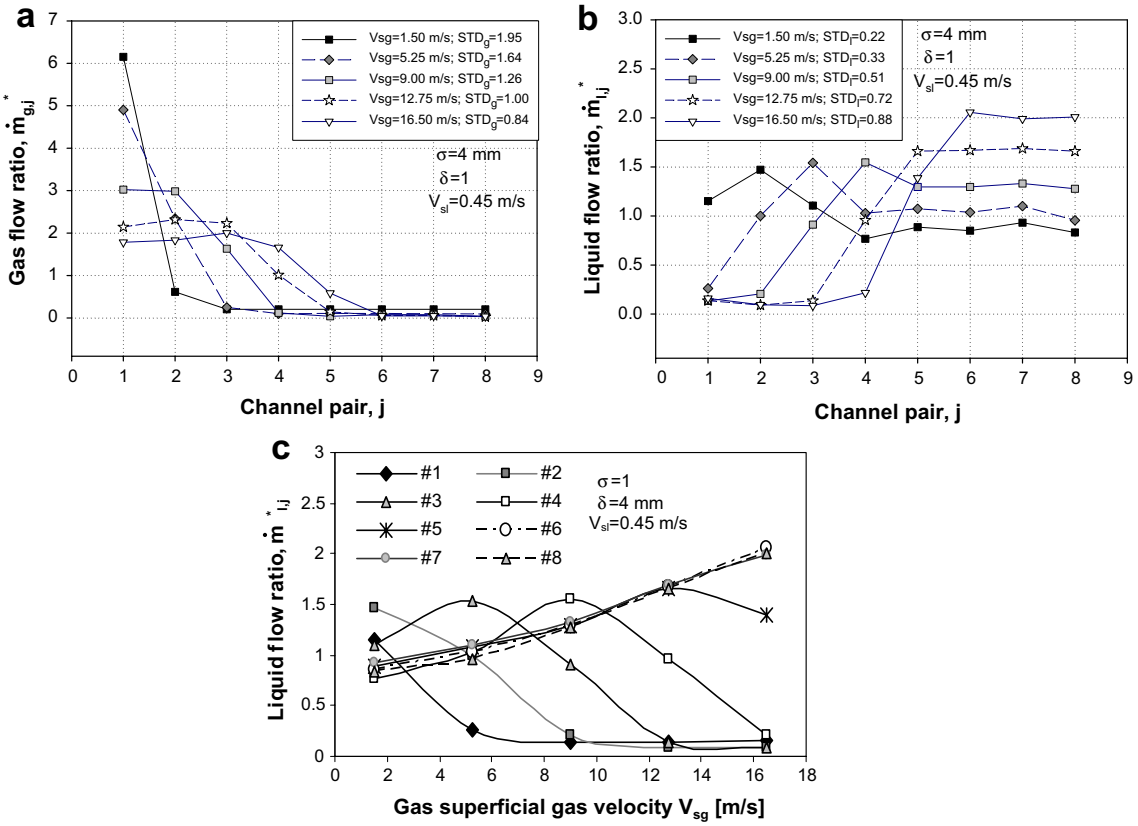

Fig. 4. Profiles of the gas flow ratio (a) and of the liquid flow ratio (b) inside the channel pairs for orifice plate diameter $\delta = 4$ mm; (c) liquid flow ratio inside different pairs of channels versus gas superficial velocity (# indicate the number of channel pair from the inlet).

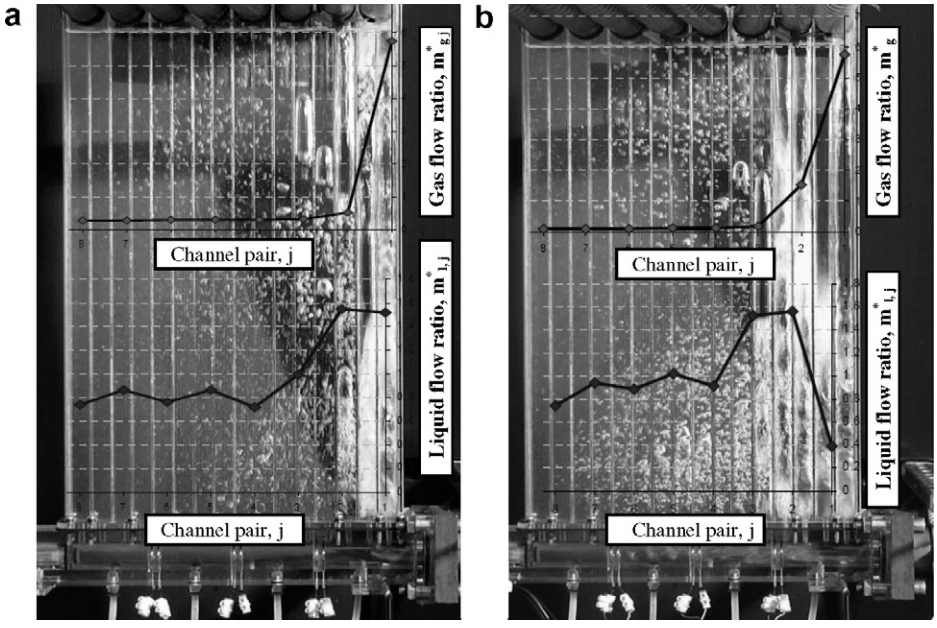

Fig. 5. Gas and liquid flow ratio inside the channel pairs for low liquid and gas superficial velocities ($V_{sl} = 0.45$ m/s, $V_{sg} = 1.50$ m/s (a) and 5.25 m/s (b)). Orifice plate diameter $\delta = 4$ mm.

phase tended to feed only the last channels. All these behaviours are represented in Fig. 6a and b and also in the images in Fig. 7.

The gas and liquid flow ratio profiles shown in Fig. 6a and b have been described by many authors as typical of horizontal headers connected to vertical upward channels. However, when the liquid and the gas superficial velocities are quite low, the liquid flow ratio exhibits a maximum in the channels located in the upstream part of the header (Figs. 4 and 5). This last behaviour was also observed by Horiki and Osakabe (1999) in their study on horizontal protruding-type headers in which the water flow was contaminated with bubbles.

The effects of the operating conditions on gas and liquid flow ratio profiles can be represented synthetically in terms of STD for both phases. As shown in Fig. 8, on increasing the gas flow rate, the gas STD_g decreased, for any liquid superficial velocity examined, thus reducing the mal-distribution of the gas phase. By contrast, the liquid phase distribution tended to worsen when the gas superficial velocity increased, and the water

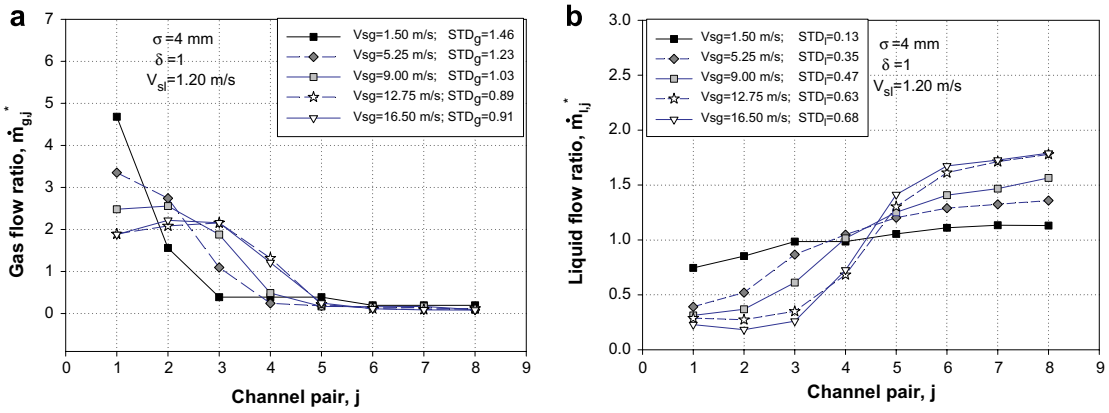

Fig. 6. Profiles of the gas flow ratio (a) and of the liquid flow ratio (b) inside the channel pairs for orifice plate diameter $\delta = 4$ mm and for a liquid superficial velocity of 1.20 m/s.

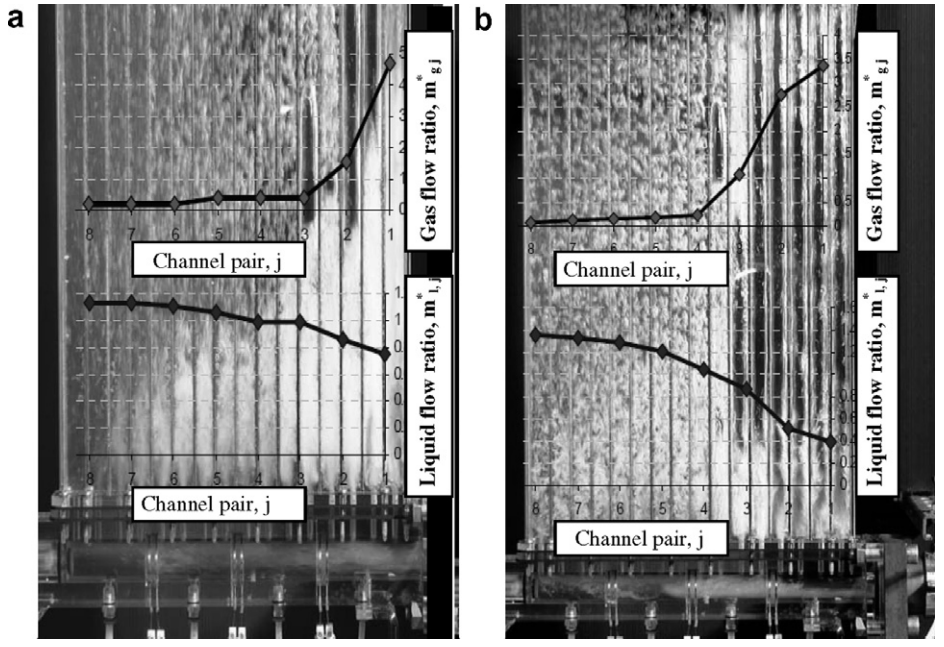

Fig. 7. Gas and liquid flow ratio inside the channel pairs for high gas and liquid superficial velocities ($V_{sl} = 1.20$ m/s, $V_{sg} = 1.50$ (a) and 5.25 m/s (b)). Orifice plate diameter $\delta = 4$ mm.

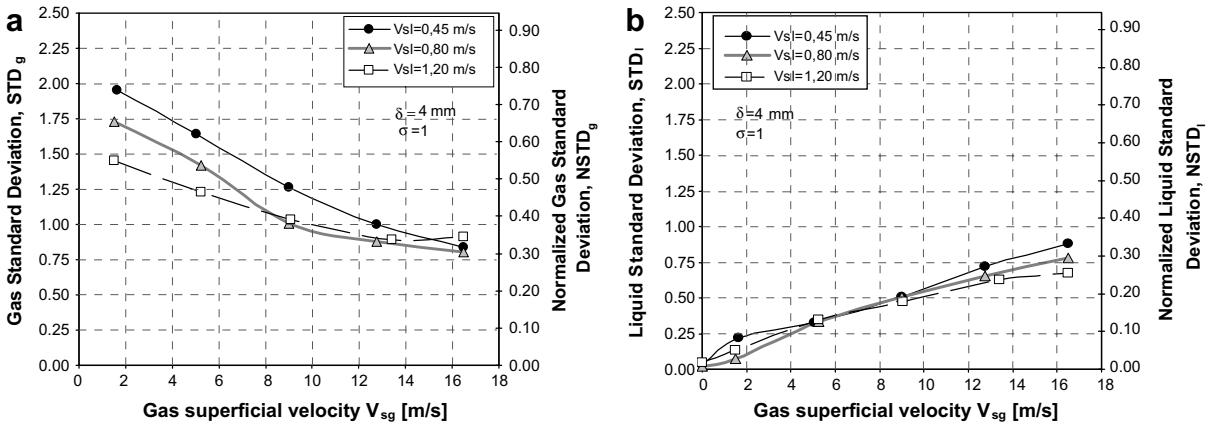

Fig. 8. Effects of the superficial velocities on the liquid (a) and gas (b) standard deviations.

tended to feed only the last channels. As a result of these effects, the quality mixture STD decreases as both liquid and gas superficial velocities increase.

Finally, the effects of the operating conditions described above were generally observed for all the other orifice plate configurations. However, as the ratio A_R was reduced, the occurrence of the maximum of the liquid flow ratio in the upstream or intermediate channels was observed for a wider range of liquid and gas flow rates. For $A_R = 10.56$ ($\delta = 2$ mm) the maximum was observed in the range $V_{sl} \leqslant 0.25$ m/s, $V_{sg} \leqslant 1.35$ m/s; for $A_R = 1.17$ ($\delta = 6$ mm) however, it was observed in the wider range $V_{sl} \leqslant 0.45$ m/s, $V_{sg} \leqslant 12.75$ m/s.

4.2. Effects of the diameter of the orifices connecting the distributor to the channels

Reducing the orifice diameter generally had a typical dual effect: the gas mal-distributions diminished, while the liquid mal-distributions tended to increase. Concerning the liquid flow ratio, at low gas superficial velocities and small orifice diameters, the entrainment of the water into the first channels tended to disappear; at higher gas superficial velocities, the shift of the liquid toward the last channels became more evident. As an example, the diagrams in Fig. 9 show a comparison between the results obtained with orifices of 2, 3, 4 and 6 mm, for the same values of gas and liquid superficial velocity ($V_{sl} = 0.45$ m/s, $V_{sg} = 1.50$ and 5.25 m/s).

The effects of orifice diameter δ and header-channel distribution area ratio A_R on the gas and liquid distributions are also well represented by the standard deviation STD_g and STD_l. As shown in Fig. 10, while enlarging the orifice diameter generally improved the liquid uniformity inside the channels, the liquid standard deviation STD_l always increased as the gas superficial velocity rose, as already seen in Fig. 8. On the other hand, the gas standard deviation STD_g showed an opposite behaviour: its value increased as the orifice diameter increased and as the gas flow rate decreased. Similar STD profiles were also observed at higher liquid velocities ($V_{sl} = 0.80$ and 1.20 m/s), but the effect of the orifice diameter was less marked.

4.3. Effects of the presence of an orifice nozzle upstream of the distributor

The presence of a nozzle at the inlet of the distributor significantly modified phase distribution into the parallel channels. The main effect of such a restriction was to produce a jet inside the distributor that modified the flow patterns.

This effect was also noticeable with regard to the liquid distribution in single-phase flow: a strong reduction of the inlet flow area ($d = 12$ m, $\sigma = (d/D)^2 = 0.21$) forced the water to the rear part of the header. A CFD analysis of the single-phase distributor, together with the connected upstream duct, was carried out by means of the *Fluent 6.1*© code using first-order approximation for derivatives and Standard k–ε model for turbulence. CFD numerical results were obtained for different orifice nozzle diameters. The comparison between CDF results and the corresponding experimental data is reported in Fig. 11 with reference to the liquid flow,

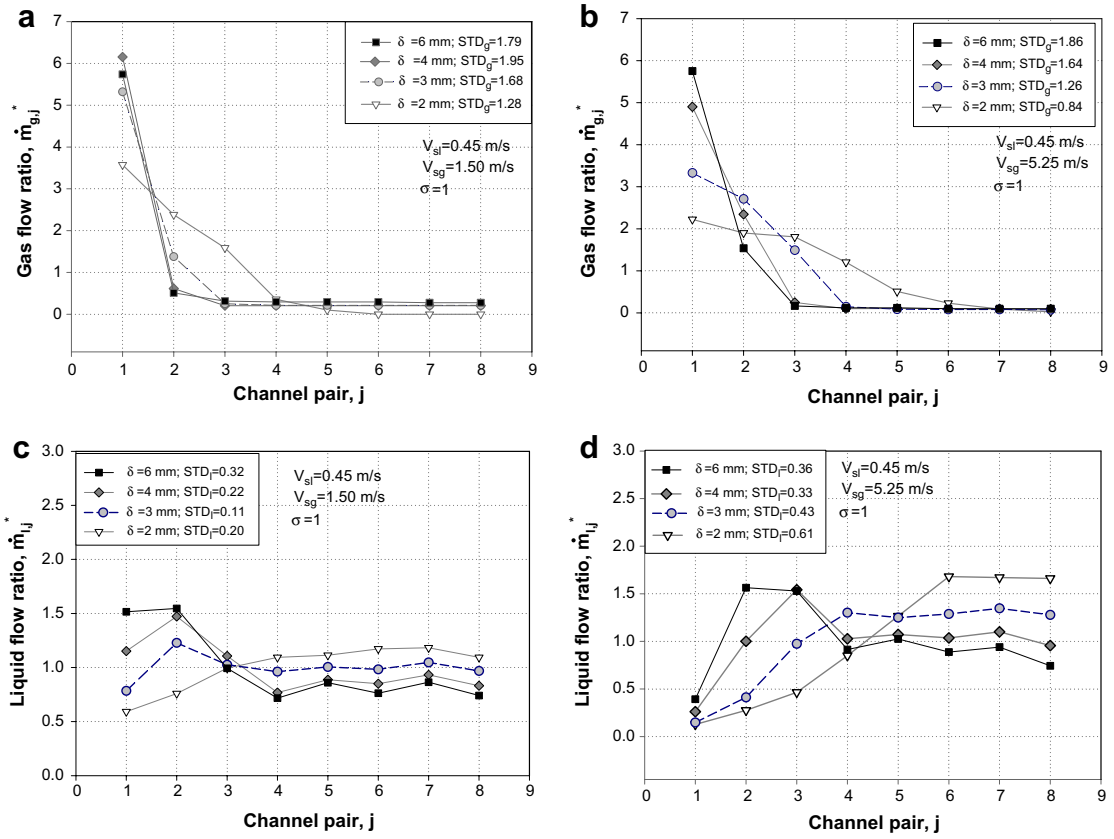

Fig. 9. Profiles of the gas flow ratio (a, b) and of the liquid flow ratio (c, d) inside the channel pairs for different orifice plate diameters ($\delta = 2$, 3, 4 and 6 mm).

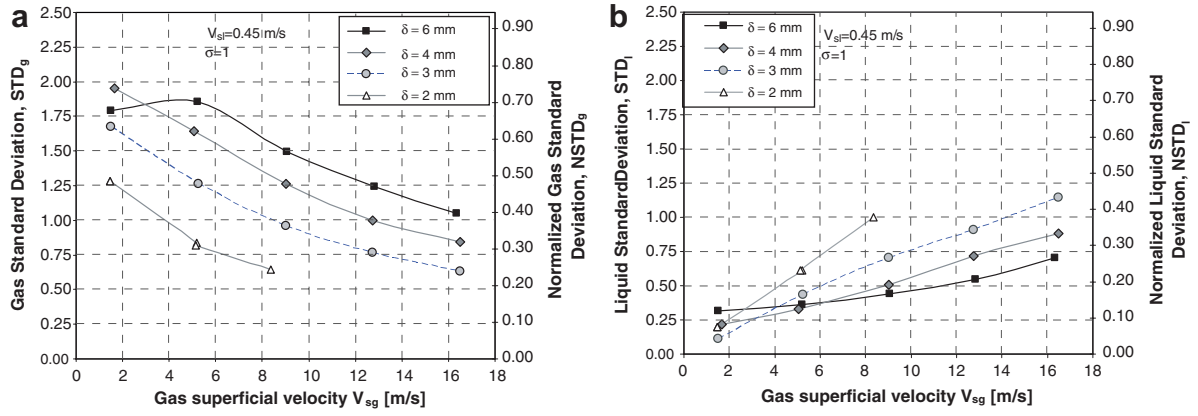

Fig. 10. Gas and liquid standard deviations for plate orifice of different diameters as a function of gas superficial velocity.

with or without the presence of an inlet orifice nozzle. It can be observed that the agreement between measurements and simulations is quite good, and that the presence of the upstream restriction produces no benefit on the single-phase distribution; on the contrary it can worsen the distribution.

When the header was fed with a two-phase flow mixture, the orifice nozzle produced a jet, the main effect of which was to change the local phase distribution and, at the same time, to increase the two-phase flow momentum at the header.

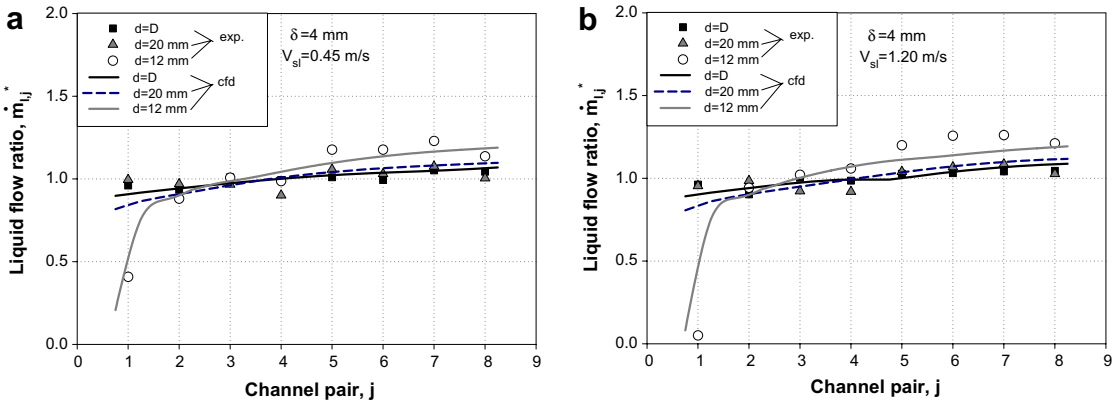

Fig. 11. Liquid flow ratio distributions with and without upstream orifice nozzle during liquid single-phase flow ($d = 12$, 20 mm). Experimental and CFD distributions.

Diagrams in Fig. 12 show the gas and liquid flow ratio inside the channels as a function of the gas superficial velocity; the operating conditions are the same as in Fig. 4c. In particular, Fig. 12a and b refer to an upstream orifice nozzle of 12 mm ($\sigma = 0.21$); Fig. 12c and d show results without an orifice nozzle ($\sigma = 1$).

The effect of the inlet restriction was to improve the distribution of the gas among the channels as an effect of the increased local gas velocity. The distribution of the liquid flow ratio also improved for the first channels,

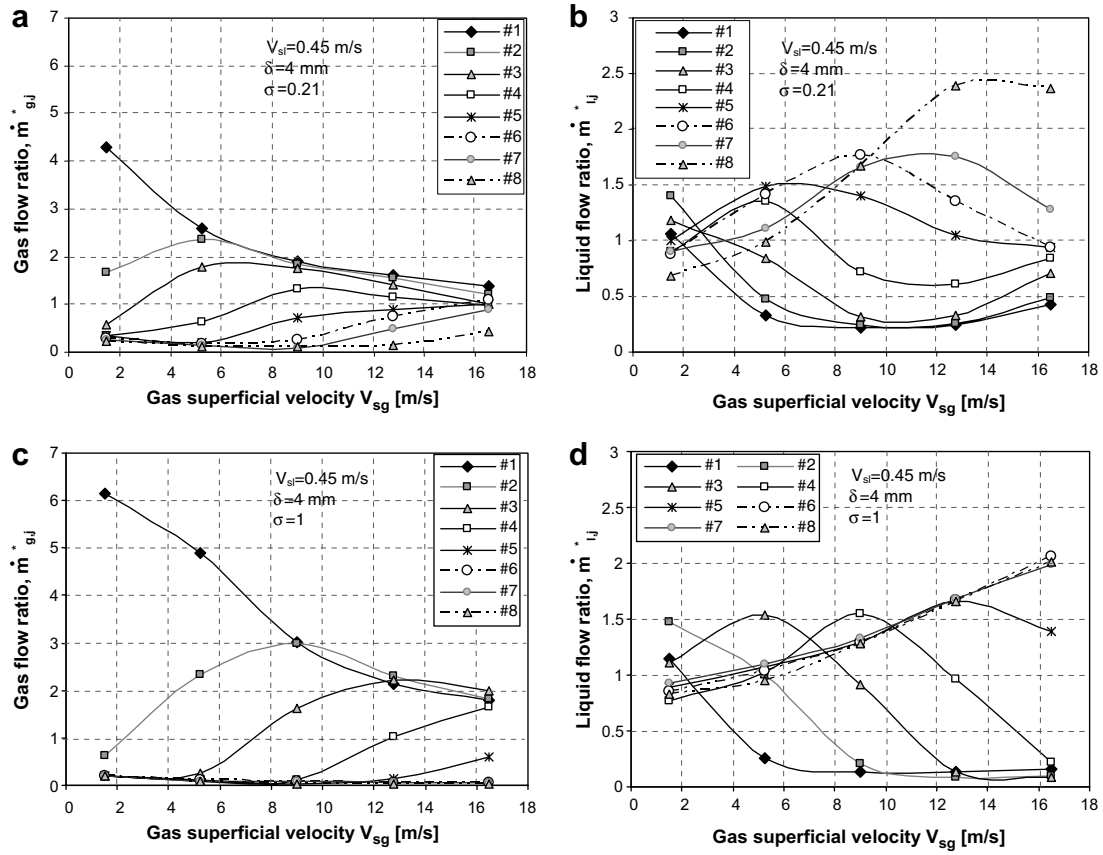

Fig. 12. Gas and liquid flow ratios versus the gas superficial velocity: (a, b) with upstream orifice nozzle of 12 mm ($\sigma = 0.21$); (c, d) without nozzle ($\sigma = 1$).

especially at low gas superficial velocities. Analysis of standard deviation functions referred to the liquid showed that the presence of the orifice nozzle improved the liquid distribution at the highest gas superficial velocities; for intermediate values of V_{sg} the effect was either to improve or to worsen the liquid distribution, depending on the value of superficial liquid velocity and on the nozzle diameter.

The presence of an inlet nozzle, at higher superficial gas velocity ($V_{sg} = 16.50$ m/s), significantly improved the flow distributions of both gas and liquid phases, as shown in Fig. 12, for $V_{sl} = 0.45$ m/s, and as calculated in terms of the standard deviation STD – without nozzle, $STD_l = 0.88$ and $STD_g = 0.84$; – with 12 mm nozzle, $STD_l = 0.58$ and $STD_g = 0.26$. These results justify the wide use of inlet nozzles by PHE manufactures of heat exchangers to empirically adjust the flow rate distribution for a certain value of the power unit and for certain ranges of the mixture quality.

To better describe what happens inside the header when an inlet nozzle is inserted, some measurements were taken by means of impedance probes able to measure the instantaneous value of the cross-sectional void fraction (Fossa, 2001). Four probes were positioned as indicated in Fig. 2: S1 (upstream of the header) and S2, S3 and S4 (inside the header). Fig. 13 reports some results in terms of probability density function (PDF) of void fraction for $V_{sl} = 1.20$ m/s and $V_{sg} = 5.25$ m/s. The results were obtained with orifice diameter $\delta = 4$ mm and with a nozzle of either $d = 20$ mm (Fig. 13a) or $d = 12$ mm (Fig. 13b) at the inlet of the header. In both cases, the flow pattern at the inlet of the header (probe S1) can be considered intermittent, with de-aerated liquid slugs. A greater inlet restriction (Fig. 13b) seems to produce a transition to the annular regime inside the header, at the level of the first pair of channels (probe S2) and to increase the time-averaged void fraction $\bar{\alpha}$ inside the central zone of the header. As a result, the gas distribution improved: the STD_g decreased from 1.00 to 0.80 when the area restriction was decreased from $\sigma = 0.59$ ($d = 20$ mm) to $\sigma = 0.21$ ($d = 12$ mm). The effect of a greater restriction in this case was to worsen the liquid distribution, with STD_l increasing from 0.35

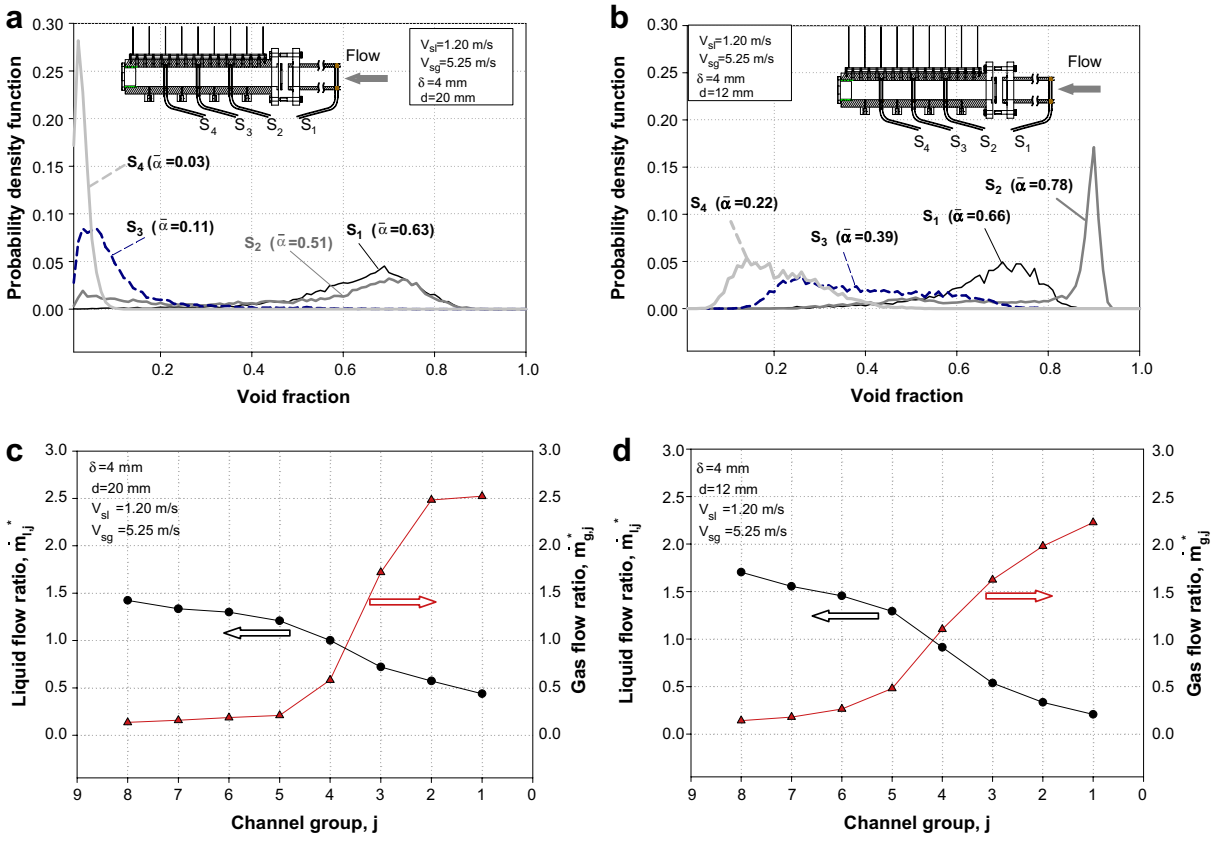

Fig. 13. Effects of the nozzle diameter on void fraction PDFs upstream of the header and inside it and on liquid and gas flow ratios.

to 0.55. Only at higher liquid superficial velocity did both STD_g and STD_l decrease as a consequence of inlet nozzle restriction, as reported in Fig. 12.

5. Conclusions

The present paper reports the results of several experiments carried out on a horizontal cylindrical two-phase flow header supplying sixteen vertical channels. The flow inside the vertical channels was upward. Measurements of air–water flow rate distributions were taken for a number of operating conditions and for different geometrical configurations. In particular, we analysed the effects of nozzles and of orifices placed upstream of the header and connecting it to the channels, respectively. Video pictures were taken to visualize different flow patterns inside the distributor and two-phase flow distributions in the range from intermittent to annular flow. Time varying, cross-sectional void fraction data were also examined in order to characterise the two-phase flow patterns at the inlet and inside the header itself.

Experimental results showed that the operating conditions exerted a strong influence on the structure of the two-phase flow pattern inside the header and therefore on the flow distribution to the channels. Different gas and liquid flow ratio profiles along the header and different values of gas and liquid STD were observed as a function of gas and liquid inlet superficial velocities.

Such distributions can be significantly modified by varying the ratio A_R between the header cross-sectional area and total inlet cross-sectional area of channels, i.e. by varying the orifice diameter. On increasing the area ratio, by reducing the diameter of the orifice connecting the header to the channels, the gas distribution improved and standard deviation STD_g decreased, while the liquid standard deviation STD_l, markedly increased especially for high gas superficial velocities.

The presence of a nozzle at the inlet of the distributor also significantly modified the flow rate distribution to the parallel channels. The main effect of a restriction was to produce a jet inside the distributor that modified the internal flow pattern. The effect of the restriction was to improve the distribution of the gas among the channels by increasing the local gas superficial velocity. The analysis of the STD of the liquid flow ratio showed that the presence of the nozzle produced a better distribution at higher gas superficial velocities; however, for intermediate V_{sg} values, a worsening effect was sometimes observed, depending on the superficial liquid velocity and on the nozzle diameter.

The results obtained confirm the complexity of two-phase flow distribution phenomena and the difficulty of designing a header–multiple channel system able to achieve even distributions for a given range of operating conditions. Indeed, the whole experimental activity indicated that the flow pattern at the inlet port and flow rate distribution inside each vertical channel depend on the interaction of several coexisting factors: gas and liquid superficial velocity, area restriction ratio, presence and geometry of an inlet nozzle, and other geometrical parameters (inlet port length and diameter, orifice diameter). The combined use of orifices at the inlet of the multiple channels and nozzles at the distributor inlet seems to be a promising way to improve flow rate uniformity inside parallel channels over a specified range of gas and liquid inlet superficial velocities. From these results it seems possible, provided that extensive experimental data are available, to find proper area ratio values A_R and σ able to minimise the STD values over a given range of gas and liquid superficial velocities.

Acknowledgement

This work has been undertaken within the Project COFIN 2004098758 supported by the Italian Ministry of University and Scientific Research (MIUR) and by the University of Genoa.

References

Acrivos, Babcock D.B., Pigford, R.L., 1959. Flow distribution in manifolds. Chem. Eng. Sci. 10, 112–125.

Bajura, R.A., Jones, E.H., 1976. Flow distributions manifolds. J. Fluids Eng., 654–666.

Bassiouny, M.K., Martin, H., 1984. Flow distribution and pressure drop in plate heat exchangers – I. Chem. Eng. Sci. 39 (4), 693–700.

Beaver, A., Hrnjak, P.S., Yin, J., Bullard, C.W., 2000. Effects of distribution in headers of microchannel evaporators on transcritical CO2 heat pump performance. In: Proceedings of the ASME Advanced Energy Systems Division, Orlando, FL, AES, 40, pp. 55–64.

Bernoux, P., Mercier, P., Lebouchè, M., 2001. Two-phase flow distribution in a compact heat exchanger. In: Proceeding of the Third International Conference on Compact Heat Exchanger, Davos, pp. 347–352.

Cho, H., Cho, K., Kim, Y.S., 2003. Mass flow rate distribution and phase separation of R-22 in multi-microchannel tubes under adiabatic condition. In: First International Conference on Microchannels and Minichannels, Rochester, New York, USA, pp. 1060–1065.

Fei, P., Cantrak, D., Hrnjak, P., 2002. Refrigerant Distribution in the inlet Header of Plate Evaporators. SAE paper 2002-01-0948, World Congress.

Fei, P., Hrnjak, P.S., 2004. Adiabatic Developing Two-Phase Refrigerant Flow in Manifolds of Heat Exchangers. ACRC Technical Report TR-225, University of Illinois at Urbana Champaign.

Fossa, M., 2001. Gas–liquid distribution in the developing region of horizontal intermittent flows. ASME J. Fluids Eng. 123, 71–80.

Fossa, M., Guglielmini, G., 2002. Pressure drop and void fraction profiles during horizontal flow through thin and thick orifices. J. Exp. Therm. Fluid Sci. 26 (5), 513–523.

Guglielmini, G., 2006. Two-phase flow distribution to parallel channels in compact heat exchangers. In: Proceedings of the 24th National UIT Heat Transfer Conference, Naples, Italy, May 21–23, pp. 13–22.

Horiki, S., Osakabe, M., 1999. Water flow distribution in horizontal protruding-type header contaminated with bubbles. Proc. ASME Heat Transfer Div. 2, 69–76.

Hrnjak, P., 2004. Developing adiabatic two-phase flow in headers – distribution issue in parallel flow microchannel heat exchangers. Heat Transfer Eng. 25 (3), 61–68.

Kim, S., Choi, E., Cho, Y.I., 1995. The effect of header shapes on the flow distribution in a manifold for electric packaging applications. Int. Commun. Heat Mass Transfer 22 (3), 329–341.

Kim, N.-H., Sin, T.-R., 2006. Two-phase flow distribution of air–water annular flow in a parallel flow heat exchanger. Int. J. Multiphase Flow 32, 1340–1353.

Lee, S.Y., 2006. Flow distribution behaviour in condensers and evaporators. In: Proceedings of the 13th International Heat Transfer Conference, Paper KN-08, Sydney, Australia, August 13–18.

Lee, J.K., Lee, S.Y., 2004. Distribution of two phase annular flow at header-channel junctions. J. Exp. Therm. Fluid Sci. 28, 217–222.

Li, G., Braun, J.E., Groll, E.A., Frankel, S., Wang, Z., 2002a. Application of CFD models to two-phase flow in refrigerant distributors, R12-6. In: Purdue Refrig. Conf.

Li, G., Braun, J.E., Groll, E.A., Frankel, S., Wang, Z., 2002b. Evaluating the performance of refrigerant flow distributors, R12-6. In: Purdue Refrig. Conf.

Mueller, A.C., 1987. Effects of some type of maldistribution on the performance of heat exchangers. Heat Transfer Eng. 8 (2), 75–86.

Mueller, A.C., Chiou, J.P., 1988. Review of various types of flow maldistribution in heat exchangers. Heat Transfer Eng. 9 (2), 36–50.

Osakabe, M., Hamada, T., Horiki, S., 1999. Water flow distribution in horizontal header contamined with bubbles. Int. J. Multiphase Flow 25, 827–840.

Probhakara Rao, B., Sunden, B., Das, S.K., 2005. An experimental and theoretical investigation on the effect of flow maldistribution on the thermal performance of plate heat exchangers. J. Heat Transfer 127, 332–343.

Rong, X., Kawaji, M., Burgers, J.G., 1996. Gas–Liquid and Flow Rate Distributions in Single End Tank Evaporator Plates. SAE Technical Paper Series, Paper no. 960375.

Taitel, Y., Dukler, A.E., 1976. A model for predicting flow regime transitions in horizontal and near-horizontal gas–liquid flow. AIChE J. 22, 47.

Taitel, Y., Pustylnik, L., Tshuva, M., Barnea, D., 2003. Flow distribution of gas and liquid in parallel pipes. Int. J. Multiphase Flow 29, 1193–1202.

Tomkins, D.M., Yoo, T., Hrnjak, P., Newell, T., Cho, K., 2002. Flow distribution and pressure drop in micro-channel manifolds. In: 9th International Refrigeration and Air Conditioning Conference, Paper R6-4, Purdue, W. Lafayette, IN, July 16–19.

Vist, S., Pettersen, J., 2004. Two phase flow distribution in compact heat exchangers manifolds. J. Exp. Therm. Fluid Sci. 28, 209–215.

Watanabe, M., Katsuta, M., Nagata, K., 1995. General characteristics of two-phase flow distribution in a multipass tube. Heat Transfer – Jpn. Res. 24 (1), 32–44.

Webb, R.L., Chung, K., 2005. Two-phase flow distribution to tubes of parallel flow air-cooled heat exchangers. Heat Transfer Eng. 26 (4), 3–18.

Yin, J.M., Bullard, C.W., Hrnjak, P.S., 2002. Single-phase pressure drop measurements in a micro-channel heat exchanger. Heat Transfer Eng. 23 (3), 3–12.

Zuber, N., Jones, O.C., 1975. The interrelation between void fraction fluctuations and flow patterns, two-phase flow. Int. J. Multiphase Flow 2, 273–306.